Precison Navigation with AD-HOC Autosurvey using UltraWideBand Two-Way Ranging Network

Brandon Dewberry & Alan Petroff
Time Domain
Huntsville, Alabama USA
brandon.dewberry@timedomain.com
alan.petroff@timedomain.com

***Abstract*—A local navigation system is constructed from Ultra Wideband (UWB) ranging radios participating in a Time Division Multiple Access (TDMA) network. The radios share a pre-configured slotmap allowing each node a duration with which to simultaneously measure a distance and broadcast data. The static "anchor" nodes range to one another, in turn. The dynamic "mobile" nodes range to the anchors, in turn. During each slot the ranging radio also broadcasts its last range measurement using an "Echo Last Range" (ELR) protocol. A Graphical User Interface (GUI) base station, wired to any one of the nodes, gathers the ELR messages, dynamically computes the anchor polygon using Least-Squares Regression, and updates the mobile location(s) using an Extended Kalman Filter (EKF) technique. User-supplied geometric and range-targeting constraints allow improvements in accuracy and update rate. The resulting system works well indoors and through non-metallic walls, and can be quickly deployed and evaluated for accuracy, latency, and coverage. Experimental results for range accuracy, network operation and localization are described.**

Keywords—UltraWideband; Two Way Time of Flight Ranging; TDMA networks; Range Accuracy;

I. INTRODUCTION

Precision indoor Real-Time Location Systems (RTLS), especially those utilizing Time Difference of Arrival (TDOA) require heavy infrastructure setup with manual survey of anchor locations and timing calibration. As the coverage area changes or grows re-calibration is required. This burden makes them less attractive for real-time vehicle safety and cooperative operations among vehicles and nearby personnel.

Wi-Fi and Bluetooth-based indoor localization systems take advantage of infrastructure already in place, or inexpensive to add, but even with the support of Simultaneous Localization and Mapping (SLAM) the continuous-wave nature of the RF limits their absolute precision in all but the most pristine of environments. While all of these technologies benefit from the fact that they are inexpensive and ubiquitous, their ranging performance is rather coarse and do not prove reliably accurate range measurements. Systems based on measuring the received signal strength suffer when the operating environment changes. Systems based on bandwidth simply have too little bandwidth to resolve multipath. In these cases, inaccuracies on the order of multiple meters are common.

There is a rich body of research that discussions different localization approaches and that how specific applications and localization techniques drive networks architecture [1,2,3]

This paper describes a localization system designed to enable both quick, inexpensive deployment as well as precise indoor localization. This system utilizes an Impulse-Radio Ultra Wideband (IR-UWB) RF physical layer, ideal for reducing RF multipath errors. A Time Division Multiple Access (TDMA) Media Access Control (MAC) layer has been added to enable efficient range measurement and data communication. A localization solver, connected to any one or all of the nodes, provides for dynamic reconfiguration and localization based on constraints provided by the user.

II. UWB TWO WAY RANGING

A. Description of Two Way Time of Flight Ranging (TWToF)

The pulsed UWB signaling strategy has been described elsewhere [4]. Implementation details include packetization of streams of pulses with separate acquisition and payload properties. The acquisition frame is optimized for fast search and locking by a rake receiver. The payload supports modulated pulses for data transmission as well as pulses in support of equivalent-time scanning of the channel for estimation of the direct path time offset [5].

Fig. 1 provides a simplified timing diagram of the two way ranging conversation between Node 1 (which is requesting a range measurement) and Node 2 (which will respond to the request). In this example, a single pulse is used to depict the "equivalent time" estimation which actually requires the transmission of a complete packet of pulses. The figure represents full packet transmission as a single timing event $\tau_1^{(tx)}$ and represents full packet reception by the responder as a single timing event $\tau_2^{(rx)}$. The key to multipath resistance and timing precision can be seen in the received waveforms, which consist of the summation of multiple copies of the transmitted pulse after propagating through a multipath channel. Impulse UWB separates these copies allowing precise determination of the Time of Arrival (TOA) of the first arriving energy in the received signal.

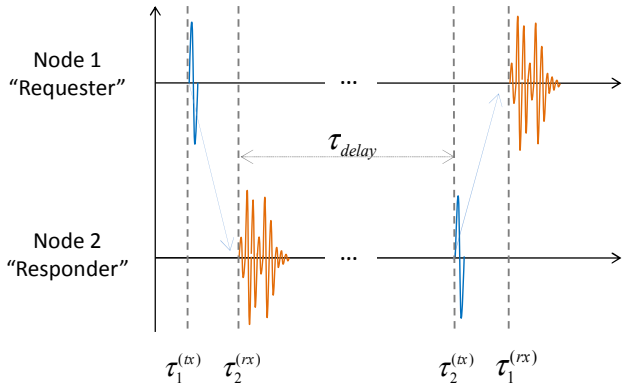

Fig. 1. The time progression of the Two-Way Time-of-Flight measurement..

The responding node will compute the TOA of the signal, delay a very precise amount of time (accurate to picoseconds) and then transmit that information to the requesting node. The requestor will compute the TOA of this response packet and then use the transmitted data to compute the range using (1).

$$\hat{r}_{1,2} = \frac{c}{2}\left(\tau_1^{(rx)} - \tau_1^{(tx)} - \tau_{delay}\right) \quad (1)$$

B. Range Error Estimation

An example of typical scans from four common environments is depicted in Fig. 2.

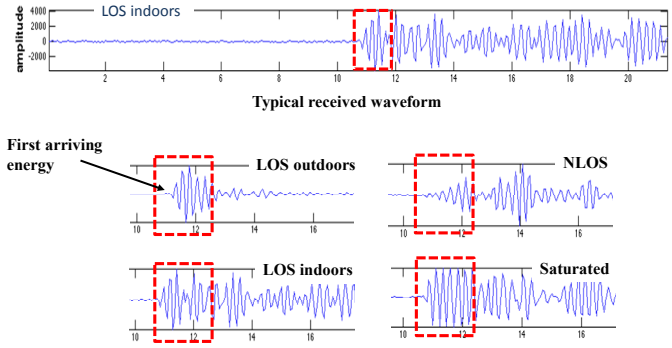

Fig. 2. A variety of scan channels and their signatures.

While the waveform envelopes of the Line-of-Sight (LOS) outdoor and LOS indoor rise times are similar (resulting in equally precise TOA and range measurements) the Non-Line of Sight (NLOS) rises much slower due to propagation through absorbing materials. The TOA event of this measurement will have more variability than the LOS examples, thus one might expect the resulting range measurement to have wider variance. Indeed, this signature variation can be quantified as a variance estimation and dynamically calculated with each range measurement. Providing a range measurement as well as a range error estimate allows inline adjustment of the Bayesian weight used by the recursive optimal EKF. This metric can also be used to form a link weight for the weighted NLS algorithm used to Autosurvey the anchor nodes [5].

Reference [6] is an excellent resource for any discussion concerning UWB ranging accuracy and propagation in complex environments. It also features an impressive reference section.

III. SYSTEM EXAMPLE

A. Example five node system

This section describes a hypothetical five-node system which will be used in later sections to illustrate the mathematics of localization.

Fig. 3 depicts a five-node system (four anchors and one mobile) used as an example for illustrating the network, anchor autosurvey, and mobile navigation discussion that follows. The network is flexible in allowing multiple various topologies, as long as adequate geometric information is available.

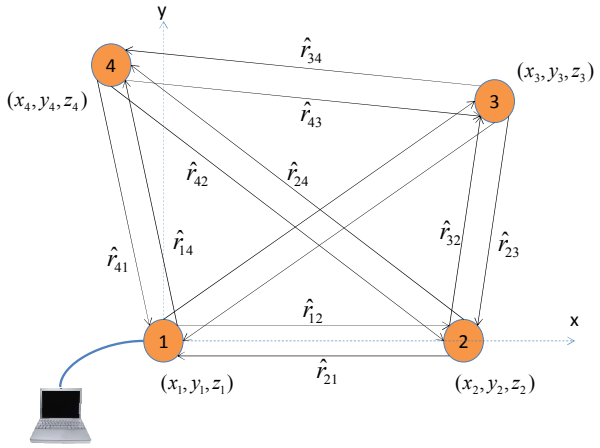

Fig. 3. Example system of a five-node navigation system.

B. Network

A contention-free Time Division Multiple Access (TDMA) time-slotted network is used to coordinate communications and range measurements. For fully mobile dynamic systems an ALOHA (randomized transmission) technique may be more applicable if the collision loss is tolerable based on short communication time and/or a small number of nodes in each neighborhood [7].

The basic mechanism of TDMA is a common network clock which is used to drive an airtime "slotmap". In addition, each node transmits its previous range measurement as data embedded in the range request packet. All nodes overhear this data and optionally provide it to a co-located host processor. This echoing of the last range (or ELR) is a useful tool for propagating information through the network.

An example of a slot map supporting four network nodes, with unique identifiers 100-103 is given in Table 1. Each slot supports a TWToF range conversation with associated ELR measurement. On completion of slot 12, the process will repeat from the slot 1.

TABLE I. EXAMPLE TDMA SLOT MAP

Slot #	Requester	Responder	ELR
1	100	101	yes
2	100	102	yes
3	100	103	yes
4	101	102	yes
5	101	103	yes
6	102	103	yes

Slot #	Requester	Responder	ELR
7	101	100	yes
8	102	100	yes
9	103	100	yes
10	102	101	yes
11	103	101	yes
12	103	102	yes

C. Nonlinear Least Squares Autosurvey

There are many trilateration methods available for localization based on distances to known target locations [8]. The best choice typically depends on the dynamics of the system. Dynamic localization typically requires a distributed/navigation approach, in which each mobile device recursively updates its own location and velocity estimate, based on partial information as it becomes available. Alternatively, static "anchor" ad-hoc localization can include a setup stage allowing a centralized approach allowing more data processing and higher accuracy.

This section provides a brief derivation of the mathematical framework involved in combining the ranges between n points into a polygon. These points are assumed to be relatively static such that the range measurements can be gathered at a single computing location. The advantage of this global recursive technique is any individual localization error is shared among all the locations. This minimizes the effects of individual range errors and the resulting propagation of registration error to the mobile units. User constraints must also be added to place the resulting polygon on a map or grid which forms the basis coordinate system.

A fully-formed polygon with n vertices contains full link distances for all $n(n\text{-}1)$ links. These measurements provide $\hat{r}_{i,j}$ in a system of equations is described by

$$\hat{r}_{i,j} = \sqrt{(x_i - x_j)^2 + (y_i - y_j)^2 + (\tilde{z}_i - \tilde{z}_j)^2}\ ,\ \{1 \le i,j \le n, i \ne j\} \quad (2)$$

These equations are re-written in a form suited for regression:

$$f_{ij} = (x_i - x_j)^2 + (y_i - y_j)^2 + (\tilde{z}_i - \tilde{z}_j)^2 - \ \hat{r}_{i,j}^2,\ \{1 \le i,j \le n, i \ne j\} \quad (3)$$

where the goal is to minimize $f_{ij} \equiv F$, a ℓx1 column vector of residuals, where $\ell = n(n-1)$ is the number of links between n nodes.

The example system depicted in Fig. 3 contains four nodes implying six links ($\ell = 6$) resulting in a system of six equations with one redundancy (only five links are required to fully define this polygon.) Thus while six link measurements will be used in regression the number of unknowns must be reduced to five from a total of twelve (x_i, y_i, z_i), $\{1 \le i \le 4\}$. External constraints are introduced to reduce the number of unknowns:

1. The node heights, $\tilde{z}_i, \{1 \le i \le 4\}$, are given as manually measured heights above a common ground plane.
2. Node 1 is designated the "origin node", $\boldsymbol{x}_1 = (x_1, y_1, z_1) = (0,0,\tilde{z}_1)$
3. Node 2 defines the x-axis, i.e. $y_2 = 0$.

The remaining unknowns form the vector $X = [x_2, x_3, y_3, x_4, y_4]'$ which will be isolated through iterative regression of the system of equations with each link measurement. Note the choice of constraints is somewhat arbitrary and can be modified to fit the external data available.

This system forms a nonlinear least squares (NLS) problem to be solved through Gauss-Newton regression [9]. Gauss-Newton requires formulation of a Jacobian/gradient matrix equation $\boldsymbol{J}(X)$ which supports iterative multidimensional minimization of the system of equations $F(\hat{r},X)$. J for this example is provided in (4) and (5).

$$\boldsymbol{J} = \begin{pmatrix} \frac{\partial f_{1,2}}{\partial x_2} & \frac{\partial f_{1,2}}{\partial x_3} & \frac{\partial f_{1,2}}{\partial y_3} & \frac{\partial f_{1,2}}{\partial x_4} & \frac{\partial f_{1,2}}{\partial y_4} \\ \frac{\partial f_{1,3}}{\partial x_2} & \frac{\partial f_{1,3}}{\partial x_3} & \frac{\partial f_{1,3}}{\partial y_3} & \frac{\partial f_{1,3}}{\partial x_4} & \frac{\partial f_{1,3}}{\partial y_4} \\ \frac{\partial f_{1,4}}{\partial x_2} & \frac{\partial f_{1,4}}{\partial x_3} & \frac{\partial f_{1,4}}{\partial y_3} & \frac{\partial f_{1,4}}{\partial x_4} & \frac{\partial f_{1,4}}{\partial y_4} \\ \frac{\partial f_{2,3}}{\partial x_2} & \frac{\partial f_{2,3}}{\partial x_3} & \frac{\partial f_{2,3}}{\partial y_3} & \frac{\partial f_{2,3}}{\partial x_4} & \frac{\partial f_{2,3}}{\partial y_4} \\ \frac{\partial f_{2,4}}{\partial x_2} & \frac{\partial f_{2,4}}{\partial x_3} & \frac{\partial f_{2,4}}{\partial y_3} & \frac{\partial f_{2,4}}{\partial x_4} & \frac{\partial f_{2,4}}{\partial y_4} \\ \frac{\partial f_{3,4}}{\partial x_2} & \frac{\partial f_{3,4}}{\partial x_3} & \frac{\partial f_{3,4}}{\partial y_3} & \frac{\partial f_{3,4}}{\partial x_4} & \frac{\partial f_{3,4}}{\partial y_4} \end{pmatrix}, \quad (4)$$

$$= \begin{pmatrix} -2(x_1 - x_2) & 0 & 0 & 0 & 0 \\ 0 & -2(x_1 - x_3) & -2(y_1 - y_3) & 0 & 0 \\ 0 & 0 & 0 & -2(x_1 - x_4) & -2(y_1 - y_4) \\ 2(x_2 - x_3) & -2(x_2 - x_2) & -2(y_2 - y_3) & 0 & 0 \\ 2(x_2 - x_4) & 0 & 0 & -2(x_2 - x_4) & -2(y_2 - y_4) \\ 0 & 2(x_3 - x_4) & 2(y_3 - y_4) & -2(x_3 - x_4) & -2(y_3 - y_4) \end{pmatrix} \quad (5)$$

A general solution to a three-dimensional, four-node system requires solving for twelve unknowns: (x_i, y_i, z_i), $\{1 \le i \le 4\}$. However, only five equations are available. Thus external constraints must be supplied. Typical examples include:

4. $\tilde{z}_i, \{1 \le i \le 4\}$ are given as manually-measured antenna heights above a common plane..
5. Designation of Node 1 to be the "origin node", $\boldsymbol{x}_1 = (x_1, y_1, z_1) = (0,0,\tilde{z}_1)$
6. Node 2 defines the x-axis: $y_2 = 0$.

The resulting the vector of unknowns is $X = [x_2, x_3, y_3, x_4, y_4]'$. Note, the choice of which variables to convert to constants is somewhat arbitrary.

A "shift vector", $\boldsymbol{H}$, is solved in each iteration of the Gauss-Newton minimization process:

$$\boldsymbol{H} = [\mathbf{J}^T \boldsymbol{W} \boldsymbol{J}]^{-1} \boldsymbol{J}^T \boldsymbol{W} F \quad (6)$$

and $\boldsymbol{W}$ is the weighting matrix with diagonal weights formed from the variances of the range measurements

$$\boldsymbol{W} = diag\left(\left[{}^1/_{\hat{\sigma}_{1,2}} \quad {}^1/_{\hat{\sigma}_{1,3}} \quad {}^1/_{\hat{\sigma}_{1,4}} \quad {}^1/_{\hat{\sigma}_{2,3}} \quad {}^1/_{\hat{\sigma}_{2,4}} \quad {}^1/_{\hat{\sigma}_{3,4}}\right]\right) \quad (7)$$

The standard deviation of error estimate $\hat{\sigma}_{i,j}$ is given by the radio with each range measurement as the Range Error Estimate (REE) discussed in the previous section. Finally, in each iteration k, the weighted NLS algorithm updates the unknowns $\hat{X} = [x_2, x_3, y_3, x_4, y_4]'$ using

$$\hat{X}^{\{k+1\}} = \hat{X}^{\{k\}} - H^k \tag{8}$$

D. Extended Kalman Filter

The mobile localization algorithm is based on a three-dimensional, sixth-order state vector x (9) and covariance matrix P (10):

$$\hat{\mathbf{x}} = \begin{bmatrix} x \\ \dot{x} \\ y \\ \dot{y} \\ z \\ \dot{z} \end{bmatrix}, \tag{9}$$

$$\mathbf{P} = \begin{bmatrix} var(x) & cov(x,\dot{x}) & cov(x,y) & cov(x,\dot{y}) & cov(x,z) & cov(x,\dot{z}) \\ cov(x,\dot{x}) & var(\dot{x}) & cov(\dot{x},y) & cov(\dot{x},\dot{y}) & cov(\dot{x},z) & cov(\dot{x},\dot{z}) \\ cov(x,y) & cov(\dot{x},y) & var(y) & cov(y,\dot{y}) & cov(y,z) & cov(y,\dot{z}) \\ cov(x,\dot{y}) & cov(\dot{x},\dot{y}) & cov(y,\dot{y}) & var(\dot{y}) & cov(\dot{y},z) & cov(\dot{y},\dot{z}) \\ cov(x,z) & cov(\dot{x},z) & cov(y,z) & cov(\dot{y},z) & var(z) & cov(x,\dot{z}) \\ cov(x,\dot{z}) & cov(\dot{x},\dot{z}) & cov(y,\dot{z}) & cov(\dot{y},\dot{z}) & cov(\dot{y},\dot{z}) & var(\dot{z}) \end{bmatrix} \tag{10}$$

Note that both these constructs will vary with time index k, which in this case has be dropped to simplify notation.

F, the system dynamics model for linear motion contains Δt, the time since the last update and Q defines the system error model. In addition Q includes σ_a, the assumed acceleration error, used as a tuning factor.

$$\mathbf{F} = \begin{bmatrix} 1 & \Delta t & 0 & 0 & 0 & 0 \\ 0 & 1 & 0 & 0 & 0 & 0 \\ 0 & 0 & 1 & \Delta t & 0 & 0 \\ 0 & 0 & 0 & 1 & 0 & 0 \\ 0 & 0 & 0 & 0 & 1 & \Delta t \\ 0 & 0 & 0 & 0 & 0 & 1 \end{bmatrix}, \tag{11}$$

$$\mathbf{Q} = \begin{bmatrix} \Delta t^2/3 & \Delta t/2 & 0 & 0 & 0 & 0 \\ \Delta t/2 & 1 & 0 & 0 & 0 & 0 \\ 0 & 0 & \Delta t^2/3 & \Delta t/2 & 0 & 0 \\ 0 & 0 & \Delta t/2 & 1 & 0 & 0 \\ 0 & 0 & 0 & 0 & \Delta t^2/3 & \Delta t/2 \\ 0 & 0 & 0 & 0 & \Delta t/2 & 1 \end{bmatrix} \tag{12}$$

The prediction phase propagates the mobile node forward and expands its covariance estimate based on the pre-configured acceleration assumption σ_a.

$$\hat{\mathbf{x}}(k+1|k) = \mathbf{F}(\Delta t)\hat{\mathbf{x}}(k) \tag{13}$$

$$\mathbf{P}(k+1|k) = \mathbf{F}(\Delta t)\mathbf{P}(k)\mathbf{F}^{-1}(\Delta t) + \mathbf{Q}(\Delta t, \sigma_a) \tag{14}$$

The update computes the modeled range and uses this to compute a linearized Jacobian observation vector. Note the localizer must use the associated anchor location (x_n, y_n, z_n):

$$\hat{r}_n(k+1) = \sqrt{(\hat{x}(k+1|k) - x_n)^2 + (\hat{y}(k+1|k) - y_n)^2 + (\hat{z}(k+1|k) - z_n)^2} \tag{15}$$

$$\mathbf{H}(k+1) = \left[\frac{(\hat{x}(k+1|k)-x_n}{\hat{r}_n(k+1)}, 0, \frac{(\hat{y}(k+1|k)-y_n}{\hat{r}_n(k+1)}, 0, \frac{(\hat{z}(k+1|k)-z_n}{\hat{r}_n(k+1)}, 0\right] \tag{16}$$

The Kalman gain is computed:

$$\mathbf{K}(k+1) = \frac{\mathbf{P}(k+1|k)\mathbf{H}^T(k+1)}{\mathbf{H}(k)\mathbf{P}(k|k-1)\mathbf{H}^T(k+1)+\sigma_r{}^2(k+1)} \tag{17}$$

Note the range measurement noise $\sigma_r{}^2(k+1)$ is the Range Error Estimate (REE) dynamically computed with each range measurement based. When this value is large, indicating a severe NLOS channel, the localizer will "lean" on the motion model. When small, the location "snaps to" the measured dimension.

The Kalman gain provides a Bayesian weight for optimal update of the state and covariance estimates. Note the new range measurement $r(k+1)$ is applied in this step:

$$\hat{\mathbf{x}}(k+1) = \hat{\mathbf{x}}(k+1|k) + \mathbf{K}(k+1)[r(k+1) - \hat{r}_n(k+1)] \tag{18}$$

$$\mathbf{P}(k+1) = \big(\mathbf{I} - \mathbf{K}(k+1)\mathbf{H}(k+1)\big)\mathbf{P}(k+1|k) \tag{19}$$

IV. Experimental Results

A. Objective and Platforms

The experiments had three objectives: demonstrate the accuracy of the individual range measurements, confirm that the TDMA network was fully operational, and confirm that the localization produced reasonable results. The experiments used the following Time Domain hardware and software platforms: P400 series UWB platforms [10,11] and the Beta version of RangeNet 1.3[12].

A key feature of the hardware is its ability to over resolve the waveform. While the received waveform can be measured with a resolution as small as 2ps, waveforms were measured at a 61ps resolution. Over resolving the waveform is important because it allows the first arriving energy to be determined through a correlation process thereby allowing range measurements to be taken with sub centimeter accuracy. This is much better 30cm accuracy implied by the 1GHz RF bandwidth.

B. TWToF range accuracy experiments

These tests focused on measuring the accuracy of the measurements over distances up to 600 meters. The reference measurement was taken with a survey grade laser based system, the Nikon DTM-550 Total Station, which has millimeter accuracy.

While measuring the accuracy of the system was straightforward, obtaining a sufficiently reliable bias measurement was difficult. It was therefore decided to focus on accuracy measurement and postpone a rigorous investigation of bias until a more robust methodology was developed. Instead of measuring the actual bias, the change in bias over distance was measured. As a result the bias estimation at short range suffers from a parallax error which diminished quickly with increasing distance.

For each of several distances, a laser range measurement was taken and compared with the average of 500 UWB range measurements attempts. This average was used to compute an estimate of the bias. The standard deviation of readings was computed and used as a measure of accuracy. Initiating a range request does not guarantee that the measurement will complete successfully. This is especially apparent when operating at maximum range. Therefore the success rate was also computed. The results are summarized in Table 2.

TABLE II. UWB RANGING PERFORMANCE VS. LASER SYSTEM

Approximate Range (m)	Laser Range (m)	Ranging Completion Rate (out of 500)	Average UWB Range (m)	Standard Deviation (cm)	Bias (cm)
40	40.2221	100%	39.7716	0.46	14.05
80	80.1861	100%	79.7839	0.22	9.22
120	120.4920	100%	120.1273	1.35	5.47
160	160.4037	99%	160.0745	0.46	1.92
200	200.4113	100%	200.0978	0.35	0.35
240	240.3625	100%	240.0502	0.25	0.23
280	280.4616	99%	280.1555	0.19	-0.39
320	320.3809	99%	320.0869	0.18	-1.6
360	360.3469	99%	360.0478	0.35	-1.09
400	399.3704	98%	399.0806	0.18	-2.02
500	500.2939	90%	499.9624	0.31	2.15
550	550.2089	92%	549.9125	0.30	-1.36
600	601.2490	56%	600.9169	0.44	2.21

There are three items of note. First, the ranging completion rate was almost 100% out to a range of 500 meters at which point the success rate deteriorated quickly. Second, the accuracy (1 standard deviation) or the range measurements is on the order of 5mm. The only exception to this rule is found at 120m reading. This point corresponds to the range at which Fresnel cancellation is occurring. Third, it was also noted that in all cases the errors in measurement were Gaussian. Consequently, averaging readings will reduce the standard deviation by the square root of the number of readings averaged. This applies to all of the measurements including those at the Fresnel cancellation point. Finally, the UWB bias error was estimated to be on the order of 2cm. At ranges less than 100m the parallax effect is quite visible. The measurement technique used to determine bias clearly needs work and will be the subject of additional tests to be performed in Spring of 2015.

C. Network descripton and performance

The P400 UWB platform has two modes of operation. It can perform simple point to point range measurements or it can operate as a network. The RangeNet network resides in the P400 platform and supports operation using either the ALOHA or TDMA protocols. Both modes support up to eleven different CDMA communication channels.

It should also be noted that it is possible to create and demonstrate networks using just the non-network mode and that such systems are normally used for navigation or localization [13,14]. However, this requires a separate host processor and a significant development effort.

RangeNet has two important features. First, all network functions (scheduling, ranging, data transmission and reporting) are performed by the P400 and operation is completely independent of a host processor. A separate host processor, such as a laptop or single board computer, is not required. However, it is useful to have at least one host processor. A host processor is used to define the P400 operating modes, establish the slot map, source and receive information. Information would include range measurements, performance statistics, and actual data packets. Second, the ELR capability enables range measurements to be broadcast through the network.

TDMA requires the maintenance of a common clock. RangeNet clock accuracy is approximately 500us and can be propagated through the system. In other words, one unit will be designated as the master and all units in the immediate range of the maser will be synchronized to the master with an accuracy of better than 1ms. This clock will also be distributed to units which are out of range of the master but within range of one of the units in the immediate vicinity of the master.

While the network can transport data, the primary objective of the system is to provide range information. Transporting more than a few dozen bytes per range attempt will consume communications bandwidth and slow the ranging network.

The performance of the TDMA network was tested using an 8 node system that operated at the highest rate possible. (~150Hz). The system operated perfectly for days without losing sync or dropping packets. The system was then operated with four CDMA channels. By carefully designing the slotmap, it was possible to demonstrate the expected fourfold increase in system capacity.

D. Localization performance

A demonstration was constructed that used three fixed nodes and one mobile. In addition, a laptop was connected through a USB port to one of the nodes. This laptop would receive range measurements from the connected node and use a MATLAB program to compute and display node location as a function of time.

On startup, the system determined the location of the nodes using the NLS localization technique. After a few seconds the solution stabilized and the fourth unit would be localized using the Kalman Filter approach and tracked as it moved relative to the fixed nodes.

The system was easy to set up and, qualitatively, performed quite well. If the mobile moved in a repeatable fashion, for instance around in fixed circle, then the reported locations were consistent with the expected result. Location accuracy was estimated to be a few cm. If the mobile moved outside the plane, then the solution in the Z axis was better than expected. While performance deteriorated as the mobile moved near or through the plane formed by the three reference nodes, it was still quite good. Outside the plane, the localization accuracy was on the order of several centimeters. When operated quite close to the plane, localization accuracy was on the order of 15cm. It was also possible to move the fixed nodes and still maintain reasonable performance.

In general, care had to be taken to insure the mobile moved slowly relative to the ranging measurement rate and that the Kalman filter constants were reasonably adjusted. Having said

that, performance of the localization algorithm was generally insensitive to settings if the ranging rate was higher than 50 Hz and the speed of the mobiles was less than one meter per second. The tradeoff between target speed, location and number of references, update rate and localization accuracy is involved but also well studied [15].

This is the logical point at which one would expect to collect quantitative data that measures performance under a set of specific circumstances. However, since the configuration was providing reasonable results, it was instead decided to increase the number of references from three to four and to increase the number of mobiles to at least two before taking the quantitative data. That effort is currently underway.

V. FUTURE EFFORTS

As previously noted, it is the intent to quantify the bias error of individual range measurements. Since the performance to date suggests that sub-centimeter performance is possible, the effect of second and third order effects is expected to become significant. For example, changes in temperature will change the circuit delay between pulse generation and the antenna feed point. Quantification of localization accuracy in a six element system is also important.

In addition, the RangeNet capabilities will be expanded in two ways. First, the slot table functionality will be increased to permit the collection of monostatic and bistatic radar returns. Second, the localization algorithms will be implemented in the P400 platform such that node locations are also reported.

Finally, there are a number of network issues associated with nodes joining or leaving the network or moving from one network to another. It is expected that simulation will be an important tool to inform the development of higher level network functionality.

VI. CONCLUSION

UWB-enabled Autosurvey can greatly increase the speed of anchor node placement and registration over manual survey approaches. The resulting anchor location accuracy can actually exceed that found by typical manual survey.

The Weighted Nonlinear Least Squares (WNLS) technique is an effective foundation method for optimally deriving relative anchor locations from range measurements. Localization errors are spread across all anchor locations. However the set of equations and unknowns must be adjusted to suit the needs of the architecture.

The Extended Kalman Filter (EKF) utilizes a Range Error Estimate (REE) derived from pulse waveform signature analysis. This improves robustness in various RF channels.

The resulting system allows both quick-deployment yet high accuracy and robustness.

REFERENCES

[1] K.K. Chintalapudi, A. Dhariwal, R. Govindan, G. Sukhatme, "Ad-hoc localization using ranging and sectoring," INFOCOM 2004. Twenty-third Annual Joint Conference of the IEEE Computer and Communications Societies , vol.4, no., pp.2662,2672 vol.4, 7-11 March 2004.

[2]T. Isokawa, S. Motomura, J. Ohtsuka, et al., "An anchor-free localization scheme with Kalman filtering in ZigBee sensor network," ISRN Sensor Networks, vol. 2013, Article ID 356231, 11 pages, 2013.

[3] N. Priyantha , H. Balakrishnan , E. Demaine, S. Teller, "Anchor-free distributed localization in sensor networks," Technical Report TR-892, MIT LCS, 2003.

[4] M.Z. Win and R.A. Scholtz, "Impulse Radio: How it Works," IEEE Communications Letters, vol.2, no. 2, pp.10-12, Jan 1998.

[5] B. Dewberry and W. Beeler, "Increased ranging capacity using Ultra Wideband direct-path pulse signal strength with dynamic recalibration," in 2012 IEEE/ION Position Location and Navigation Symposium (PLANS), pp.1013-1017, 23-26 April 2012.

[6] D. Dardari, A Conti, U. Ferner, A. Giorgetti, M.Z. Win, "Ranging with Ultrawide bandwidth signals in multipath environments," Proceedings of the IEEE, vol. 97, no.2, Feb 2009

[7] R. Binder, N. Abramson, F. Kuo, A. Okinaka, D. Wax, "ALOHA packet broadcasting – a retrospect," Proc National Computer Conference. AFIPS Press, 1975.

[8] L. Cheng, C. Wu, Y. Zhang, H. Wu, M. Li, and C. Maple, "A survey of localization in wireless sensor network," International Journal of Distributed Sensor Networks, vol. 2012, Article ID 962523, 12 pages, 2012.

[9] W. Murphy and W. Hereman, "Determination of a position in three dimensions using trilateration and approximate distances", 1995, tech. report MCS-95-07, Colorado School of Mines, Golden, CO.

[10] "Time Domain P410 Radio", Time Domain, 2011. Web. 14 Feb. 2014. http://www.timedomain.com/p400.php

[11] A. Petroff, "Multi-functional UltraWideband platform for ranging, radar and communications," Oct 2013 European Radar Conference (Nurnberg)

[12] "320-0320B RCM – RangeNet RET User Guide", Time Domain, 2015, Web, Feb 28, 2014, http://www.timedomain.com/p400.php

[13] M. Janssen, A. Busboom, U Shoon, G. von Coelln, C. Koch "A mobile open infrastructure network protocol (MOIN) for localization and data communication in UWB based wireless sensor networks", IEEE International Conference on Ultra-Wideband, 2014

[14] B. Beck and R. Baxley "Real-time, anchor free node tracking using Ultrawideband range and odometry data", IEEE International Conference on Ultra-Wideband Paris, Sept 2014

[15] G.E. Garcia, L.S. Muppirisetty, and H. Wymeersch, "On the trade-off between accuracy and delay in UWB navigation," in IEEE Communication Letters, vol. 17, no. 1, pp. 39 - 42, Jan 2013